

# NEW ADVANCES IN ELECTROMAGNETIC SCATTERING AND INVERSE SCATTERING FROM SUBSURFACE PROFILES

Chao Wu<sup>①②</sup> Liting Rao<sup>①②</sup> Shuai Cui<sup>①②</sup> Youcheng Wang<sup>①②</sup> Xiaojuan Zhang<sup>①</sup> Guangyou Fang<sup>①</sup>

<sup>①</sup>Institute of Electronics, Chinese Academy of Sciences, Beijing 100190, China

<sup>②</sup>University of Chinese Academy of Sciences, Beijing, China

## ABSTRACT

We propose a new method for bistatic scattering from hybrid subsurface profiles with multilayer rough interfaces and flat boundaries, which the fast method is firstly demonstrated by strictly theoretical formulas in the framework of classical small perturbation method (SPM) without other else approximation and assumption strategy. What is more, we can obtain general compact closed-form first-order perturbation solutions of hybrid subsurface profiles with an arbitrary number of rough and smooth interfaces, which is necessary to insure a successful inversion process. We employ improved inverse algorithms and get successful inverse process based on the proposed forward model.

**Index Terms**— Bistatic scattering, hybrid subsurface profiles, inverse algorithm, multilayer rough interfaces, small perturbation method.

## 1. INTRODUCTION

Subsurface sensing is of great interest in a variety of applications such as stratified soil, forest canopies, sand cover, oil flood on sea surface, sea ice and other natural scenes. The numerical, empirical, and analytical methods are carried out to study the scattering forward model for different natural scenes. In order to properly model the EM propagation of the radar signal in natural layered structures, the model should be multilayer rough interfaces separated by arbitrary inhomogeneous dielectric profiles, which can be close to the natural scenes. However, the higher efficiency and more accurate method for bistatic-scattering from hybrid model of multilayer rough interfaces separated by arbitrary inhomogeneous plane dielectric profiles has not been reported.

In this paper, we give the compact closed-form first-order solutions of multilayer rough interfaces separated by arbitrary inhomogeneous plane dielectric profiles employing the new method in the framework of small perturbation method (SPM) [1]. Currently, some extensions of SPM to the layered media with one rough surface have been proposed. The train of thought is to employ the existing models [2]-[4] and the concepts of the generalized

reflection/transmission coefficients to derive the solutions of the problem of multilayer rough interfaces separated by flat boundaries.

In addition, since we can obtain a simple invertible functional form of the unknown model parameters for the forward model, then the inversion problem [5] also can be derived straightforward and more efficiency. Furthermore, we will employ the improved simulated annealing to obtain the global minimize results of the cost function which is based on the difference between measured and calculated backscattering coefficients at different incident angles and measurement frequencies.

Moreover, now we use the dual-frequency SAR system to measure the scattering coefficients of bare soil in order to fully utilize this forward model proposed in this paper.

## 2. FORWARD SCATTERING SOLUTIONS

The problem considered here is the three-dimensional bistatic scattering from a hybrid layered structure with multilayered rough interfaces and flat boundaries shown in Fig.1. Each  $m$ -th rough, which is assumed to be characterized by zero-mean stationary random processes with known statistical properties are denoted by  $z = -d_m + \xi g_m(x, y)$ .

The electric and magnetic fields in each layer can be represented as a superposition of up- and down-going orthogonal polarized in the spectral domain according to the Huygens theory [6]. The electric and magnetic fields at the point  $\vec{r}$  in the region  $m$  can be expressed as follows:

$$\begin{aligned} \vec{E}_m(\vec{r}) = & \int_{-\infty}^{+\infty} d\vec{k}_\perp \{ [U_{mh}^+ \hat{h}_m(k_{mz}) + U_{mv}^+ \hat{v}_m(k_{mz})] e^{ik_{mz}z} \\ & + [U_{mh}^- \hat{h}_m(-k_{mz}) + U_{mv}^- \hat{v}_m(-k_{mz})] e^{-ik_{mz}z} \} e^{i\vec{k}_\perp \cdot \vec{r}_\perp} \end{aligned} \quad (1)$$

$$\begin{aligned} \vec{H}_m(\vec{r}) = & \frac{1}{Z_m} \int_{-\infty}^{+\infty} d\vec{k}_\perp \{ [-U_{mh}^+ \hat{v}_m(k_{mz}) + U_{mv}^+ \hat{h}_m(k_{mz})] e^{ik_{mz}z} \\ & + [-U_{mh}^- \hat{v}_m(-k_{mz}) + U_{mv}^- \hat{h}_m(-k_{mz})] e^{-ik_{mz}z} \} e^{i\vec{k}_\perp \cdot \vec{r}_\perp} \end{aligned} \quad (2)$$

We proposed a new fast method which is firstly demonstrated by strictly theoretical formulas derivation in the framework of classical small perturbation method (SPM) without other else approximation and assumption strategy, in

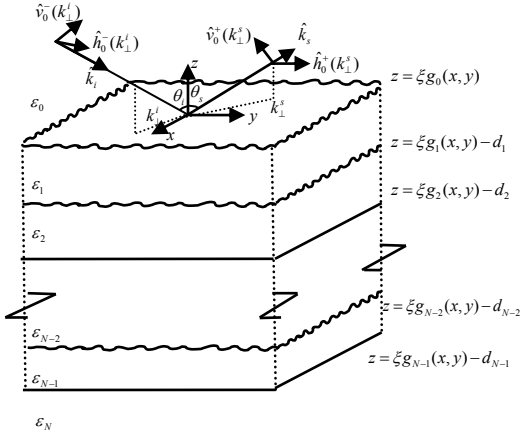


Fig. 1. Geometry for multilayer rough interfaces and flat boundaries.

order to calculate the closed-form first-order perturbation solutions of hybrid model with multilayer rough interfaces and flat boundaries.

The core of new method of calculating the problem of bistatic scattering from layered structure with multilayer rough interfaces and flat boundaries is to divided this problem into some equivalent problems in which one single interface is rough, whereas the other ones are flat, then the global bistatic scattering cross section of hybrid multilayer media can be expressed as

$$\sigma_{qp}^0 = \pi k_0^4 \sum_{n=0}^{M-1} |\tilde{\sigma}_{qp}^{n,n+1}(k_\perp^s, k_\perp^i)|^2 W_n(k_\perp^s - k_\perp^i) + \pi k_0^4 \sum_{i \neq j} \text{Re} \{ \tilde{\sigma}_{qp}^{i,i+1} (\tilde{\sigma}_{qp}^{j,j+1})^* \} W_{ij}(k_\perp^s - k_\perp^i) \quad (3)$$

with  $p, q \in \{v, h\}$  denote the incident and the scattered polarization states, respectively, and may stands for horizontal polarization ( $h$ ) or vertical polarization ( $v$ ), and the coefficient  $\tilde{\sigma}_{qp}^{n,n+1}$  is the relative to the  $p$ -polarized incident wave impinging on the structure from the upper half-space zero and to the  $q$ -polarized scattering contribution from structure into the upper half-space, originated from the rough interface between the layer  $n$  and  $n+1$ .

Now we consider the representative stratification with multilayer flat intermediate layer and two rough interfaces denoted by  $z = \xi g_1(x, y)$  and  $z = -d_1 + \xi g_2(x, y)$  respectively. This model refers to the geometry of Fig.2, which case has not been considered by other authors yet. We employ the proposed new method to derive the perturbation solutions as expressed by

$$\sigma_{pq}^{0(1)} = 4\pi k_0^2 \cos^2 \theta |\tilde{U}_{0pq}^{+(1)} + U_{0pq}^{+(1)}|^2 W(\bar{k}_\perp - \bar{k}_\perp^i) \quad (4)$$

where

$$\tilde{U}_{0hh}^{+(1)} = \frac{k_0(\varepsilon_1 - \varepsilon_0) \cos(\varphi_s - \varphi_i)}{2\varepsilon_0 \cos \theta_s} (1 + \tilde{R}_{0,1hs})(1 + \tilde{R}_{0,1hi}) E_0^h \quad (5)$$

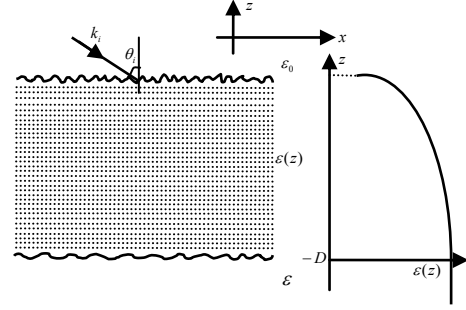


Fig. 2. Geometry for model of continuous variation permittivity media between two rough interfaces

$$\tilde{U}_{0hv}^{+(1)} = \frac{k_0(\varepsilon_1 - \varepsilon_0) \sin(\varphi_s - \varphi_i) \cos \theta_i}{2\varepsilon_0 \cos \theta_s} (1 + \tilde{R}_{0,1hs})(1 - \tilde{R}_{0,1vi}) E_0^v \quad (6)$$

$$\tilde{U}_{0vh}^{+(1)} = \frac{k_0(\varepsilon_1 - \varepsilon_0)}{2\varepsilon_0} \sin(\varphi_s - \varphi_i) (1 + \tilde{R}_{0,1hi})(1 - \tilde{R}_{0,1vs}) E_0^h \quad (7)$$

$$\tilde{U}_{0vv}^{+(1)} = \frac{k_0(\varepsilon_1 - \varepsilon_0) \sin \theta_s \sin \theta_i}{2\varepsilon_1 \cos \theta_s} (1 + \tilde{R}_{0,1vi})(1 + \tilde{R}_{0,1vs}) E_0^v - \frac{k_0(\varepsilon_1 - \varepsilon_0)}{2\varepsilon_0} \cos(\varphi_s - \varphi_i) \cos \theta_i (1 - \tilde{R}_{0,1vi})(1 - \tilde{R}_{0,1vs}) E_0^v \quad (8)$$

$$U_{0hh}^{+(1)} = \frac{k_{0z}^s}{k_{Nz}^s} (\varepsilon_{N+1} - \varepsilon_N) \cos(\phi_s - \phi_i) e^{ik_{Nz}^s d_N} \times [1 + \tilde{R}_{N,N+1}^h(k_\perp^s)] \times [1 + \tilde{R}_{N,N+1}^h(k_\perp^i)] \times \frac{\exp(\sum_{n=1}^{N-1} jk_{nz}^s \Delta_n) \prod_{n=0}^{N-1} L_{n+1,n}^h}{[1 - \tilde{R}_{N,N-1}^h(k_\perp^s) \tilde{R}_{N,N+1}^h(k_\perp^i) e^{j2k_{Nz}^s \Delta_N}]} \quad (9)$$

$$\times e^{ik_{Nz}^s d_N} \exp(\sum_{n=1}^{N-1} jk_{nz}^i \Delta_n) \prod_{n=0}^{N-1} L_{n,n+1}^h U_{0vv}^{+(1)} = \frac{k_{0z}^s}{k_{Nz}^s} \frac{\varepsilon_{N+1} - \varepsilon_N}{\varepsilon_N} \cos(\phi_s - \phi_i) e^{ik_{Nz}^s d_N} \times \frac{\exp(\sum_{n=1}^{N-1} jk_{nz}^s \Delta_n) \prod_{n=0}^{N-1} L_{n+1,n}^v}{(1 - \tilde{R}_{N,N-1}^v \times \tilde{R}_{N,N+1}^v \times e^{j2k_{Nz}^s \Delta_N})} e^{ik_{Nz}^s d_N} \times \{ [1 + \tilde{R}_{N,N+1}^v(k_\perp^s)] \} \quad (10)$$

$$\times [1 + \tilde{R}_{N,N+1}^v(k_\perp^i)] \times \frac{\varepsilon_N}{\varepsilon_{N+1}} \sin \theta_i \sin \theta_s - [1 - \tilde{R}_{N,N+1}^v(k_\perp^s)] \times [1 - \tilde{R}_{N,N+1}^v(k_\perp^i)] \cos \theta_N^i \cos \theta_N^s \} \times \exp(\sum_{n=1}^{N-1} jk_{nz}^i \Delta_n) \prod_{n=0}^{N-1} L_{n,n+1}^v$$

$$U_{0vh}^{+(1)} = -\frac{k_{0z}^s}{k_0} (\varepsilon_{N+1} - \varepsilon_N) \sin(\phi_s - \phi_i) \times e^{ik_{Nz}^s d_N} \times \frac{\exp(\sum_{n=1}^{N-1} jk_{nz}^s \Delta_n) \prod_{n=0}^{N-1} L_{n+1,n}^v}{(1 - \tilde{R}_{N,N-1}^v \times \tilde{R}_{N,N+1}^v \times e^{j2k_{Nz}^s \Delta_N})} e^{ik_{Nz}^s d_N} \quad (11)$$

$$\times [1 + \tilde{R}_{N,N+1}^v(k_\perp^i)] \times e^{ik_{Nz}^s d_N} \tilde{T}_{0,N}^h(k_\perp^i) [1 + \tilde{R}_{N,N+1}^h(k_\perp^i)]$$

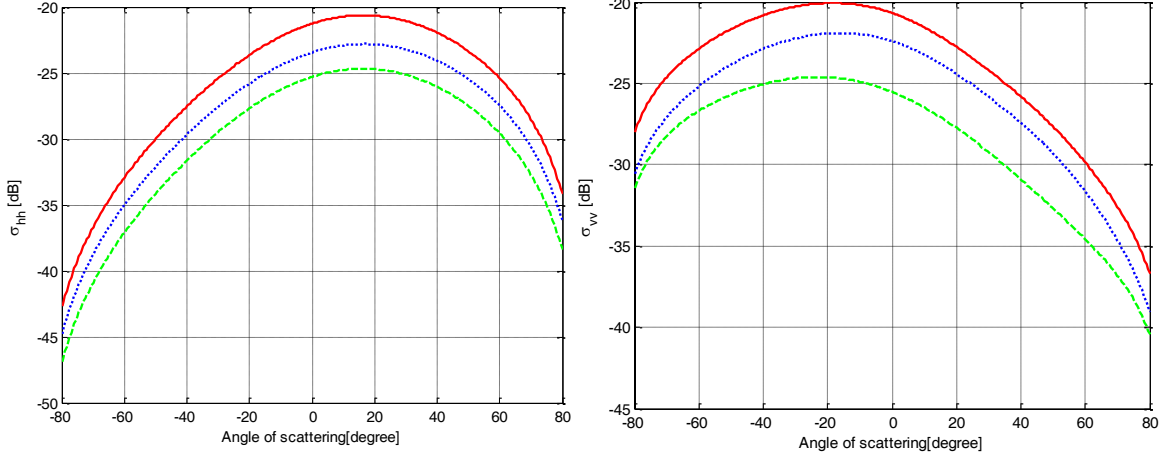


Fig.3. Bistatic scattering coefficients for multilayer structure with continuous variation permittivity media between two rough interfaces.  $\varepsilon(z) = 5.0 + 25\sqrt{z/D}$ ,  $D = \lambda$ ,  $k_0\sigma_1 = k_0\sigma_2 = 0.2$ ,  $k_0l_1 = k_0l_2 = 2.0$ ,  $f = 450$  MHz,  $\theta_0^i = 45^\circ$ ,  $\varphi_0^i = 0^\circ$  and  $\varphi_0^s = 45^\circ$ . (Blue dotted line) indicates the bistatic scattering coefficients of layered structure with multilayer flat boundaries covered by slight rough surface, (Green dashed line) shows the bistatic scattering coefficients of layered structure with rough interface covered by multilayer flat boundaries. (Red solid line) shows the global bistatic scattering coefficients in the air half-infinite space.

$$\begin{aligned}
 U_{0hv}^{+(1)} &= \frac{k_{0z}^s k_{Nz}^i \varepsilon_{N+1} - \varepsilon_N}{k_0 k_{Nz}^s \varepsilon_N} \sin(\phi_s - \phi_i) \times e^{ik_{Nz}^s d_N} \\
 &\times \frac{\exp\left(\sum_{n=1}^{N-1} jk_{nz}^s \Delta_n\right) \prod_{n=0}^{N-1} L_{n+1,n}^h}{[1 - \tilde{R}_{N,N-1}^h(k_\perp^s) \tilde{R}_{N,N+1}^h(k_\perp^s) e^{j2k_{Nz}^s \Delta_N}]} \\
 &\times [1 + \tilde{R}_{N,N+1}^h(k_\perp^s)] \times e^{ik_{Nz}^s d_N} \tilde{T}_{0,N}^v(k_\perp^i) [1 - \tilde{R}_{N,N+1}^v(k_\perp^i)]
 \end{aligned} \quad (12)$$

We assume that the two rough interfaces have properties of Gaussian function whose spectral density is given by

$$W_n(k_\perp^s - k_\perp^i) = (\sigma_n^2 l_n^2 / 4\pi) \exp(-|k_\perp^s - k_\perp^i|^2 l_n^2 / 4) \quad (13)$$

where  $l_n$  and  $\sigma_n$  are the correlation length and standard deviation of the  $n$ -th rough interface height, respectively.

In order to compare the different effects generated by each rough interface on the global scattering coefficient in the air half-infinite space, we assume that the each boundary has the same roughness with  $k_0 l_n = 2.0$  and  $k_0 \sigma_n = 0.2$  for  $n = 1, 2$ .

In Fig.3, we give the numerical results of hybrid stratification with continuous variation permittivity between two rough interfaces, which will be more close to the realistic natural scene and has not been considered by other authors yet. According to the numerical results, we can observe that the each rough interface plays an important role in the calculation of overall bistatic scattering coefficients. Therefore, when we analyze the scattering response from the natural stratified structure, we should

consider each rough interface in order to obtain the accurate results.

### 3. INVERSE SCATTERING SOLUTIONS

Since we have derived the closed-form first-order perturbative solutions of bistatic scattering from hybrid subsurface profiles with continuous variation permittivity between two rough interfaces, then we can obtain successful inversion process based on the proposed fast and accurate forward hybrid model. We have investigated two different improved inverse algorithms based on simulated annealing and genetic algorithms.

We employ the improved simulated annealing algorithm to solve the inverse problem as a global optimization problem. The cost function used in this paper is

$$\begin{aligned}
 L(X) &= \sum_{i=1}^{N_f} \sum_{j=1}^{N_\theta} \left[ \left( \frac{\sigma_{vv}^o(X; f_i, \theta_j) - d_{vv}(f_i, \theta_j)}{d_{vv}(f_i, \theta_j)} \right)^2 \right. \\
 &\quad \left. + \left( \frac{\sigma_{hh}^o(X; f_i, \theta_j) - d_{hh}(f_i, \theta_j)}{d_{hh}(f_i, \theta_j)} \right)^2 \right] \quad (14)
 \end{aligned}$$

where  $N_f$  and  $N_\theta$  are the number of frequency points and measurement angles used in measurement, respectively.

The work flow of improved simulated annealing is described as in Fig.4. We employ the improved inverse algorithm by increasing the temperature to search for the global minimum solution. The inversion parameters used in

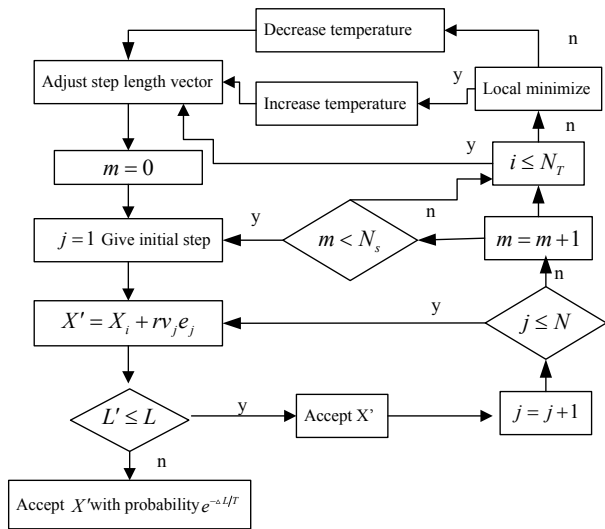


Fig.4. The work flow of improved simulated annealing algorithm

Table I  
Inverse initial parameters

$T_0$	$N_s$	$N_T$	$Re_T^k$	$Inc_T$	$\delta$	$\epsilon$	$N_\epsilon$
100000	20	100	$0.95^k$	1.20	$10^{-12}$	$10^{-10}$	10

the inverse algorithm are  $T_0$ ,  $N_s$ ,  $N_T$ ,  $Re_T^k$ ,  $Inc_T$ ,  $\delta$ ,  $\epsilon$ , and  $N_\epsilon$  introduced in table I.

#### 4. CONCLUSION

The new approach can obtain a more accurately closed-form first-order perturbation solution of hybrid subsurface profile with multilayer rough interfaces and flat boundaries. Furthermore, we can obtain more accurate inverse results employing the improved inversion algorithms with input Gaussian noise. A general explicit closed-form higher order solution for the problem of scattering from layered structure with an arbitrary number of rough interfaces is not available in the literature yet, and it will be highly desirable. In the future work, we will focus on the derivation of high order perturbation solutions [7] and analyze the physical meanings. In addition, now we use the dual-frequency SAR system to investigate electromagnetic wave scattering from the forest and vegetable canopies of natural scenes and obtain successful inversion processes.

#### 5. ACKNOWLEDGMENTS

This work is supported by the National High Technology Research and Development Program of China (863 Program under Grant No. 2009AA12Z132) and the National Natural

Science Foundation of China (Grant 61172017 and Grant 60890071-01).

#### 6. REFERENCES

- [1] L. Tsang, J. A. Kong, and R. T. Shin, *Theory of Microwave Remote Sensing*. New York: Wiley, 1985.
- [2] I. M. Fuks, "Wave diffraction by a rough boundary of an arbitrary plane-layered medium," *IEEE Trans. Antennas Propag.*, vol. 49, no. 4, pp. 630-639, Apr. 2001.
- [3] Azadegan, R.; Sarabandi, K., "Analytical formulation of the scattering by a slightly rough dielectric boundary, covered with a homogenous dielectric layer," *Antennas and Propagation Society International Symposium, 2003. IEEE*, vol.3, no., pp. 420- 423, June, 2003.
- [4] Z. Lin, X. Zhang, and G. Fang, "Theoretical model of electromagnetic scattering from 3D multi-layer dielectric media with slightly rough surfaces," *Progress In Electromagnetics Research*, Vol. 96, pp. 37-62, 2009.
- [5] Tabatabaenejad, A.; Moghaddam, M., "Radar Retrieval of Surface and Deep Soil Moisture and Effect of Moisture Profile on Inversion Accuracy," *Geoscience and Remote Sensing Letters, IEEE*, vol.8, no.3, pp.478-482, May 2011.
- [6] A. Tabatabaenejad; M. Moghaddam, "Bistatic scattering from three-dimensional layered rough surfaces," *Geoscience and Remote Sensing, IEEE Transactions on*, vol.44, no.8, pp.2102-2114, Aug. 2006.
- [7] Demir, M.A.; Johnson, J.T.; Zajdel, T.J., "A Study of the Fourth-Order Small Perturbation Method for Scattering From Two-Layer Rough Surfaces," *Geoscience and Remote Sensing, IEEE Transactions on*, vol.50, no.9, pp.3374,3382, Sept. 2012.